Synthesis and structural characterizations of tris (hydroxymethyl) aminomethane complexes with group IIA metals

Lamia A. Albedair

Dept. of Chemistry, College of Science,
Princess Nourah Bint Abdulrahman University,
Riyadh 11671, Saudi Arabia

Corresponding author: lamiaalbedair@yahoo.com

Abstract

Herein, this article aimed to investigate the tendency of tris(hydroxymethyl) aminomethane (THAM) to form stable complexes with group IIA metals. Four new colorless solid complexes of group IIA metals [Ba(II), Ca(II), Sr(II), and Mg(II)] with THAM were prepared and well characterized. The chemical reactions between-group IIA metals and THAM were conducted by the stoichiometry of 2:1 (Ligand: Metal ion) at 65 °C and pH of ~ 8.5. Under these conditions, the THAM molecule ($C_4H_{11}NO_3$) was deprotonated and converted to the ($C_4H_{10}NO_3^-$; L^-) chelate with the metal ions. The structures of these complexes were suggested by UV-visible, IR, Raman and ^{1}H NMR spectroscopies and other physicochemical and analytical methods (elemental analysis, thermogravimetry, and SEM). The results shows that the general composition of the complexes obtained with Ba(II), Ca(II), Sr(II), and Mg(II) ions are $[BaL_2(H_2O)_2]$, $[CaL_2(H_2O)_2]\cdot 2H_2O$, $[SrL_2(H_2O)_2]$, and $[MgL_2(H_2O)_2]\cdot 4H_2O$, respectively, and in all complexes, the geometry was octahedral.

Keywords: Group IIA metals; spectral analysis; thermogravimetry; tris(hydroxymethyl) aminomethane.

1. Introduction

The structure of tris(hydroxymethyl)aminomethane (THAM) which is shown in Figure 1, is a small organic molecule that exists as a colorless crystalline powder with a melting point of 175-176°C and chemical formula ($C_4H_{11}NO_3$) (121.14 g/mol). THAM has a several synonyms, such as Tris, Tris base, Tris buffer, Trisaminol, Trometamol, THAM, and Trizma. THAM is structurally related to the amino alcohol group that consists of one amino group and three hydroxyl groups. It is considered an alkalizing agent that is preferred over Na_2CO_3. THAM has several applications in physiology, biology, medicine, and biochemistry [Bubb *et al*., 1995]. It is widely used biochemically as a buffer for several biochemical processes [Brignac & Mo, 1975; Hayashi *et al*., 1981; Lundblad & Macdonald, 2010; Albishri & Marwani, 2016; El-Dissouky *et al*., 2020] and used clinically to reverse acidosis [Murakami *et al*., 2016; Kallet *et al*., 2000; Weber *et al*., 2000; Nahas *et al*., 1998]. Several THAM Schiff base derivatives showed a broad spectrum of biological activity, like anti-inflammatory, antifungal, antihistamine, anticancer, and anti-tumor effects. Several works reported the crystal structures of some THAM Schiff base ligands [Tatar *et al*., 2005; Odabasoglu *et al*., 2003; Asgedom *et al*., 1995].

The coordination chemistry of metal-based and metallodrug compounds is attracting considerable interest from pharmacists and chemists because these compounds may have a significant application in many important fields such as biology, pharmacology, and medicine to catalysis and material sciences and they can be used to design more biologically active drugs [Tella *et al.*, 2019; Mohammed *et al.*, 2014; Alessio, 2011; Tarafder *et al.*, 2001; Vakili *et al.*, 2021; Ali *et al.*, 2021]. Several metal-based compounds have been proven to possess potential biological activities, like antibacterial, antifungal, antiviral, and anticancer activities. For example, several platinum-based compounds have utility in cancer therapy for treating several solid tumors, like bladder, ovarian, and testicular cancers [Khan *et al.*, 2019; Sayadi *et al.*, 2019; Cao *et al.*, 2017; Tavares *et al.*, 2017; Singh *et al.*, 2016; Saleem *et al.*, 2013; Trudu *et al.*, 2015; Crisóstomo-Lucas *et al.*, 2015; Pagoto *et al.*, 2015; Muhammad & Guo, 2014; Mjos & Orvig 2014; Abdel-Rahman *et al.*, 2014; Guidi *et al.*, 2013; Abdel Ghani & Mansour, 2011; Dabrowiak, 2017; Hambley, 2001; Köpf-Maier, 1994]. However, drug resistance and adverse side effects have limited the effectiveness and applications of several metal-based drugs [Qin *et al.*, 2019; Dominelli *et al.*, 2018; Meng *et al.*, 2016; Hu *et al.*, 2016; Lai *et al.*, 2015; Dasari & Tchounwou 2014; Galluzzi *et al.*, 2012; Maheswari *et al.*, 2008]. Furthermore, the occurrence and fate of antibiotic residues in the environment and the extensive overuse of antibiotics caused, an increased bacterial drug resistance [Howse *et al.*, 2019; Deng *et al.*, 2019; Dai *et al.*, 2018; Walsh *et al.*, 2016]. The Global Review of Antimicrobial Resistance issued by the WHO in 2016 reported that drug-resistant infections will cause the death of 700,000 people every year [WHO, 2016]. Therefore, there is an urgent need to discover and design new metal-based compounds with the potential efficiency to overcome drug resistance and extend over the antimicrobial/anticancer spectrum with fewer side effects.

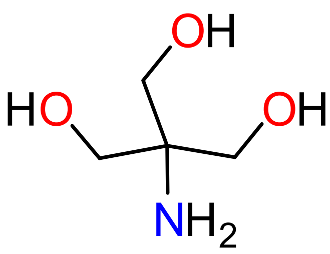

Fig. 1. Molecular structure of THAM.

Synthesizing new metal complexes may play an interesting role in the development of effective metal-based drugs. Herein, we reported the synthesis and characterization of four new products of THAM with the metal ions of Group II [Ba(II), Ca(II), Sr(II), and Mg(II)] to throw more light and provides new insights on the complexation tendency and chelation behavior of THAM towards metals. The work is separated into two sections:

(i) Synthesis of the THAM complexes:

The complexes were prepared by reacting THAM with the Ba(II), Ca(II), Sr(II) and Mg(II) ions in MeOH:H_2O solvent with a 1:2 (Metal: Ligand) ratio at 65°C.

(ii) Chemical and physical characterizations:

The spectroscopic and physicochemical techniques: CHN elemental analysis, Raman, UV-visible, ^{1}H NMR, and IR spectroscopies; SEM; and thermogravimetry were used to characterize the obtained complexes.

2. Experimental

2.1 Materials

Commercially available materials were used as received without further modification. These were bought from commercial sources (Merck and Fulka chemical companies). Tris(hydroxymethyl)aminomethane (THAM); 121.14 g/mol; purity ≥ 99.8%), $SrCl_2 \cdot 6H_2O$ (266.62 g/mol; purity 99%), $BaCl_2 \cdot 2H_2O$ (244.26g/mol; purity 99.99%), $CaCl_2$ (110.98 g/mol; purity 99.99%), $MgCl_2$ (95.21 g/mol; purity ≥ 98%), and HPLC-grade methanol were of analytical grade chemicals and were used as bought. Water purification unit (Milli-Q) was used to generate the pure deionized water for the preparation of solutions.

2.2 Synthesis

The THAM (2.0 mmol) was dissolved in 25 mL MeOH, then added gradually to an aqueous solution containing 1.0 mmol (20 mL) of the respective metal chloride salt [Ba(II), Ca(II), Sr(II), and Mg(II)]. The pH of the four solutions was adjusted to~8-9 using 5% ammonia solution, then the solutions were refluxed at 65°C under stirring for 30 minutes. After that, the four solutions were slow cooled gradually and left overnight at room temperature affording colorless precipitates. Filtration, washing two times with MeOH, and subsequent drying in vacuum for 48h yielded the pure products as colorless powders. The products were next characterized by spectroscopies (^{1}H NMR, Raman, IR, and UV-visible) as well as thermal and elemental analyses.

2.3 Methods

The UV-visible, ^{1}H NMR, Raman and IR spectra of the synthesized complexes were collected by Perkin-Elmer Lambda 25 UV/Vis spectrophotometer, Bruker DRX-250 spectrometer, Bruker FT-Raman spectrophotometer, and Shimadzu FT-IR spectrophotometer at room temperature, respectively.
The thermal and elemental data of the synthesized complexes were collected using Shimadzu TGA-50H thermal analyzer and Perkin-Elmer 2400CHN elemental analyzer, respectively. Surface morphologies of the synthesized complexes were pictured using Quanta FEG 250 SEM instrument.

3. Results and discussion

3.1 Composition and UV-visible spectra

The Ba (II), Ca (II), Sr (II), and Mg (II) chloride salts were dissolved in deionized water, where THAM was dissolved in MeOH solvent. No precipitates were seen when the methanolic solution of THAM ($C_4H_{11}NO_3$) was mixed with each aqueous solution of chloride salts. When the pH of each mixture reached ~ 8.5 by adding ammonia solution (5%), one OH group in the THAM ($C_4H_{11}NO_3$) ligand is deprotonated and converted to the ($C_4H_{10}NO_3^-$; L^-) chelate. All Ba(II), Ca(II), Sr(II), and Mg(II) ions formed a colorless product with L^- chelate, and the elemental analyses data for these products are:

i) $[MgL_2(H_2O)_2]\cdot 4H_2O$ complex:
Gross formula, $C_8H_{32}N_2O_{12}Mg$; Molecular weight, 372.63 g mol^{-1}; Elemental results: calc. (found) for C, 25.76% (25.58); H, 8.59% (8.31); N, 7.51% (7.73); Mg, 6.52% (6.77).

ii) $[CaL_2(H_2O)_2]\cdot 2H_2O$ complex:
Gross formula, $C_8H_{28}N_2O_{10}Ca$; Molecular weight, 352.38 g mol^{-1}; Elemental results: calc. (found) for C, 27.24% (27.43); H, 7.95% (7.73); N, 7.95% (8.17); Ca, 11.35% (11.16).

iii) $[SrL_2(H_2O)_2]$ complex:
Gross formula, $C_8H_{24}N_2O_8Sr$; Molecular weight, 363.89 g mol^{-1}; Elemental results: calc. (found) for C, 26.38% (26.23); H, 6.60% (6.36); N, 7.70% (7.49); Sr, 24.08% (24.35).

iv) $[BaL_2(H_2O)_2]$ complex:
Gross formula, $C_8H_{24}N_2O_8Ba$; Molecular weight, 413.60 g mol^{-1}; Elemental results: calc.(found) for C, 23.21% (23.39); H, 5.80% (5.55); N, 6.77% (7.03); Ba, 33.20% (33.40).

These data indicated that the reaction stoichiometry is 2:1 (L^-: Metal ion), which suggested that the general composition of the complexes obtained with Ba(II), Ca(II), Sr(II) and Mg(II)ions are $[BaL_2(H_2O)_2]$, $[CaL_2(H_2O)_2]\cdot 2H_2O$, $[SrL_2(H_2O)_2]$, and $[MgL_2(H_2O)_2]\cdot 4H_2O$, respectively, UV-visible spectra of the complexes were recorded over the 200-1000 nm wavelength range, showed that all the complexes gave one sharp and intense band with the wavenumber range from 300 to 350 nm. All the observed bands had one sharp head centered at 305 nm. This band may be assignable to the M→L charge transfer transitions. The band becomes more broad and strong in intensity in complexes of Mg(II) and Ba(II) ions, and much broad and very strong in intensity in a complex of Sr(II) ion.

3.2 Vibrational spectroscopy

The IR spectrum of each complex was scanned in the wavenumber range 400-4000 cm^{-1} and displayed in Figure 2. The band assignments for the important IR bands in free THAM and the complexes are given below:

IR data (cm^{-1}) for free THAM: 3351 ν(O–H), 3195 ν(N–H), 2938 ν(C–H), 1545 δ_{def}(N–H), 1462 δ_{sciss}(CH_2),1400 δ(O–H), 1292 ν(C–N), 1215 ν(C–C), 1150 δ_{rock}(CH_2), 1039 ν(C–O), and 780 δ_{wag}(CH_2).

IR data (cm^{-1}) for $[MgL_2(H_2O)_2]\cdot 4H_2O$ complex: 3325 ν(O–H), 3185 ν(N–H), 2977-2824 ν(CH_2), 1623 δ_b(H_2O), 1543 δ_{def}(N–H), 1460 δ_{sciss}(CH_2), 1393 δ(O–H), 1295 ν(C–N), 1220

ν(C–C),1153 $\delta_{rock}(CH_2)$,1027 ν(C–O),760 $\delta_{wag}(CH_2)$, 666$\delta_w(H_2O)$, 594 $\delta_t(H_2O)$, and 540 ν(Mg–O).
IR data (cm^{-1}) for $[CaL_2(H_2O)_2]\cdot 2H_2O$ complex: 3317ν(O–H), 3188ν(N–H), 2932-2824 $\nu(CH_2)$, 1629 $\delta_b(H_2O)$, 1547 δ_{def}(N–H), 1458 $\delta_{sciss}(CH_2)$, 1399 δ(O–H), 1293 ν(C–N), 1221 ν(C–C),1172 $\delta_{rock}(CH_2)$,1025 ν(C–O),790 $\delta_{wag}(CH_2)$, 660$\delta_w(H_2O)$, 600 $\delta_t(H_2O)$, and 542 ν(Ca–O).

IR data (cm^{-1}) for $[SrL_2(H_2O)_2]$ complex: 3318 ν(O–H), 3090 ν(N–H), 2975-2856 $\nu(CH_2)$, 1627 $\delta_b(H_2O)$, 1546 δ_{def}(N–H), 1450 $\delta_{sciss}(CH_2)$, 1410 δ(O–H), 1290 ν(C–N), 1227 ν(C–C), 1166 $\delta_{rock}(CH_2)$, 1023 ν(C–O), 753 $\delta_{wag}(CH_2)$, 665 $\delta_w(H_2O)$, 612 $\delta_t(H_2O)$, and 536 ν(Sr–O).
IR data (cm^{-1}) for $[BaL_2(H_2O)_2]$ complex: 3320 ν(O–H), 3187 ν(N–H), 2929-2800 $\nu(CH_2)$, 1632 $\delta_b(H_2O)$, 1545 δ_{def}(N–H), 1452 $\delta_{sciss}(CH_2)$, 1400 δ(O–H), 1291 ν(C–N), 1212 ν(C–C), 1154 $\delta_{rock}(CH_2)$, 1025 ν(C–O), 785 $\delta_{wag}(CH_2)$, 667 $\delta_w(H_2O)$, 608 $\delta_t(H_2O)$, and 520 ν(Ba–O).

Free THAM showed several distinguished absorption bands in its IR spectrum [Chen *et al.*, 2018]. Two extraordinarily strong and broad bands located at 3351 cm^{-1} and 3195 cm^{-1} were attributed to the vibrations of ν(O–H) and ν(N–H), respectively. A group of medium and sharp bands appears within the range 1600–1200 cm^{-1}, exactly at 1589 cm^{-1}, 1462cm^{-1}, 1292 cm^{-1} and 1215 cm^{-1}, were resulted from the δ_{def}(N–H), $\delta_{sciss}(CH_2)$, ν(C–N) and ν(C–C)vibrations, respectively. Band with very strong intensity and medium in broadening was located at 1034 cm^{-1} and was attributed to the ν(C–C) vibrations. When THAM complexed with Mg(II), Sr(II), Ba(II), and Ca(II) ions, the intensity and broadening of the bands due to the ν(N–H) and ν(O–H) vibrations were decreased. The frequency of the ν(O–H) vibrations was significantly shifted from 3351 cm^{-1} in the free THAM to 3325-3317 cm^{-1} in the complexes, where the frequency of the ν(N–H) vibrations was slightly shifted from 3195 cm^{-1} in the free THAM to 3190-3185 cm^{-1} in the complexes. The band of ν(C–O) occurs near 1039 cm^{-1} in the free THAM and was moved to a lower frequency in the complexes (1027-1023 cm^{-1}). The bands attributed to the δ_{def}(N–H) and ν(C–N) vibrations, remained in the same position as observed in the free THAM, along with the slight shifts in the ν(N–H) vibrations, which means that NH_2 group do not participate in the complexation. Coordinated water molecules exhibits four angular deformation motion around 1630 cm^{-1}, 851 cm^{-1}, 645 cm^{-1} and 582 cm^{-1}attributed to the δ_b(bend), δ_r(rock), δ_w(wag) and δ_t(twist) vibrations, respectively [Deacon & Phillips, 1980].

Only the band due to the δ_r(rock)vibration was not detected in the spectrum of each complex due to the overlapping of this band with other vibrational bands. The $\delta_b(H_2O)$ vibration appeared within the range of 1632-1623 cm^{-1}, that of the $\delta_w(H_2O)$ vibration appeared within the range of 667-660 cm^{-1}, while the vibration of $\delta_t(H_2O)$ was found within the range of 612-594 cm^{-1}. The weak bands noticed in the range of 540-520 cm^{-1} could be attributed to the ν(M-O) in the complexes. Figure 3 illustrates the laser Raman spectra of free THAM, and the complexes scanned in the wavenumber region 50-400 cm^{-1}.

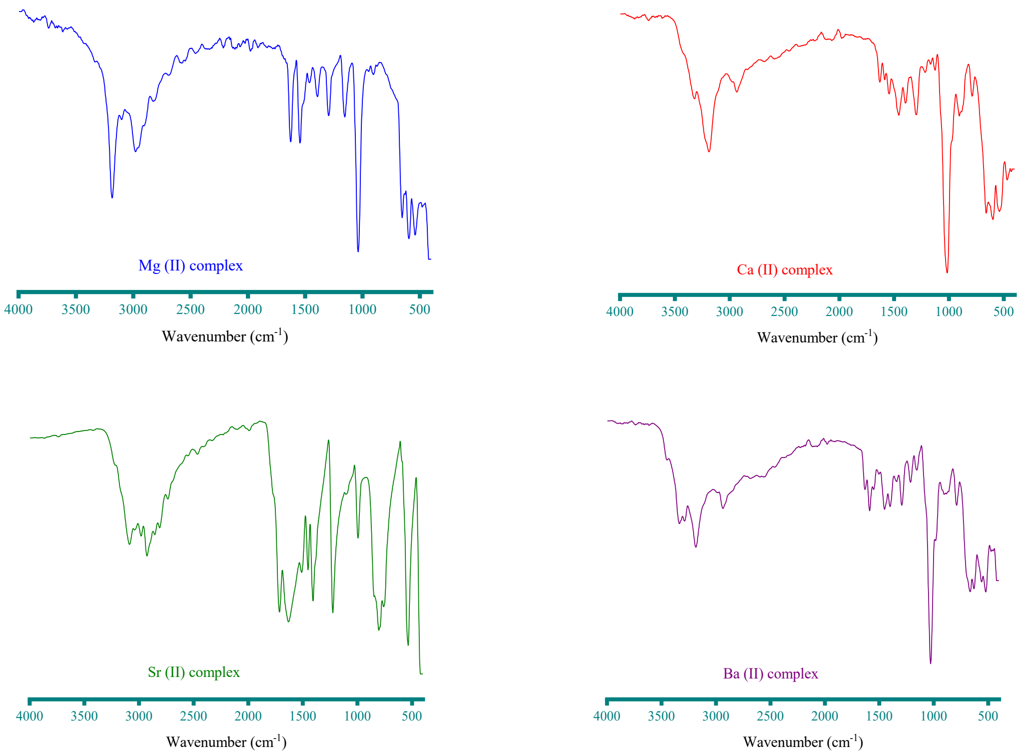

Fig. 2. IR spectra of the Ba(II), Ca(II), Sr(II),and Mg(II)complexes.

The Raman spectrum of free THAM showed four sharp and very strong bands at 1471 cm^{-1}, 1258 cm^{-1}, 1071 cm^{-1}, and 804 cm^{-1} resulting from the $\delta_{sciss}(CH_2)$, ν(C–N), ν(C–O) and $\delta_{wag}(CH_2)$ vibrations, respectively. Also, THAM shows a strong and broadband around 2945-2850 cm^{-1} assigned to the ν(C–H) vibrations. The medium and sharp band located at 3287 cm^{-1} could be assigned to the ν(O–H) vibration. In the Raman spectra of the complexes (Figure 3), the $\delta_{sciss}(CH_2)$, ν(C–N), ν(C–O) and $\delta_{wag}(CH_2)$ vibrational bands have been registered in the region 1466-1464 cm^{-1}, 1270-1255 cm^{-1}, 1050-1045 cm^{-1}, and 800-758 cm^{-1}, respectively. Based on elemental and vibrational spectral results, proposed structures of the synthesized complexes were given in Figure 4.

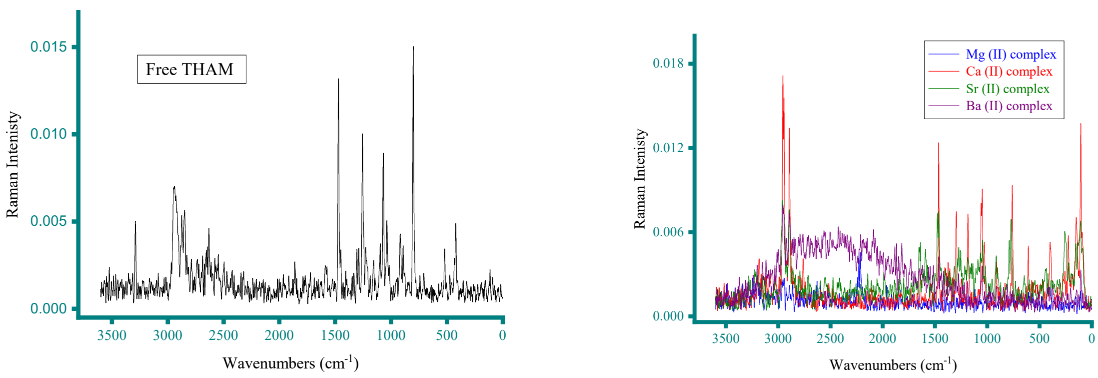

Fig. 3. Laser Raman spectra of free THAM, Ba(II), Ca(II), Sr(II),and Mg(II)complexes.

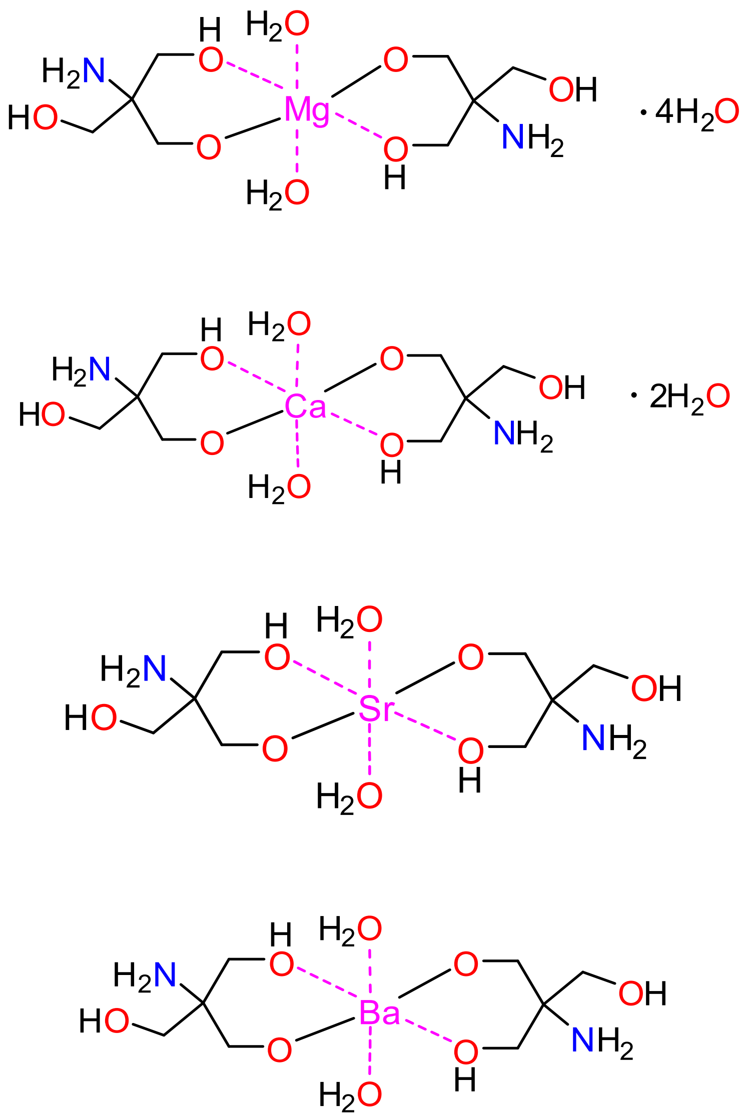

Fig. 4. Proposed chemical structures of Ba(II), Sr(II), Ca(II), and Mg(II)complex.

3.3 [1]H NMR spectroscopy

The ^{1}H NMR spectrum (DMSO-d_6) of free THAM and Ba(II) complex has been obtained at room temperature, where their chemical shifts were listed in Table 1. The resultant data of free THAM were: δ = 2.58 (s, 6H, $3CH_2$), 3.48 (s, 3H, 3OH), 7.64 (s, 2H, NH_2). The resultant data of Ba(II) complex were: δ = 2.57 (s, 12H, $6CH_2$), 3.45 (s, 4H, 4OH), 7.83 (s, 4H, $2NH_2$). Free THAM produced three signals in the 2.58-7.64 range, and all these signals were detected in the spectrum of the complex with Ba(II) ion. In the spectrum of free THAM, the protons of CH_2, OH and NH_2 groups resonated at 2.58, 3.48, and 7.64 ppm, respectively. In the spectrum of Ba(II) complex, the protons of OH, and CH_2 groups were represented slightly up-field shifts. The NH_2 protons were undergone down-field shifted and exhibited a definite singlet at 7.83 ppm. The protons of coordinated water molecules showed a broad signal at 3.52 ppm.

Table 1. The ^{1}H NMR data (ppm) of free THAM and Ba(II) complex.

Compound	C*H*$_2$ (s, 6H) methylene group	O*H* (s, 3H) OH group	N*H*$_2$ (s, 2H) NH_2group
Free THAM	2.58	3.48	7.64
Ba(II) complex	2.57	3.45	7.83

3.4 Thermogravimetry

The Compositions and structures of the complexes were confirmed by thermogravimetry. Figure 5 presents the thermograms of the free THAM, Ba(II), Ca(II), Sr(II), and Mg(II) complex. The obtained thermograms enabled the following observations:

i) The free THAM was thermally stable up to ~ 180 °C. After complexation resulted in a new Mg(II) compound with decreasing the stability to ~ 120 °C. Complexation of THAM with the Ba(II) and Sr(II) ions led to un-stable complexes, these complexes start to decompose at ~ 30 °C

ii) Complexation of THAM with Ca(II) ion formed a highly stable complex. After losing the lattice water molecules at around 80 °C, the complex remained thermally stable up to ~ 240 °C.

iii) Complexes of Mg(II) and Ca(II) ions are stable at room temperature and can be stored without any degradation.

iv) Free THAM, and the complexes with Mg(II) and Ca(II) ions were decomposed in a one-stage degradation step in the temperature range of 180-320 °C, 120-400 °C and 240-625°C, respectively. While the complexes with Ba(II) and Sr(II) ions were decomposed in two-stage degradation step in the temperature range of 30-320 °C, and 320-800 °C for Ba(II) complex, and in the temperature range of 30-300 °C and 300-800 °C for Sr(II) complex.

v) The decompositions of complexes were almost completed leaving MgO for Mg(II) complex, $BaCO_3$, $SrCO_3$, and $CaCO_3$for other complexes as the final decomposition products. All these products were contaminated with some residual carbons.

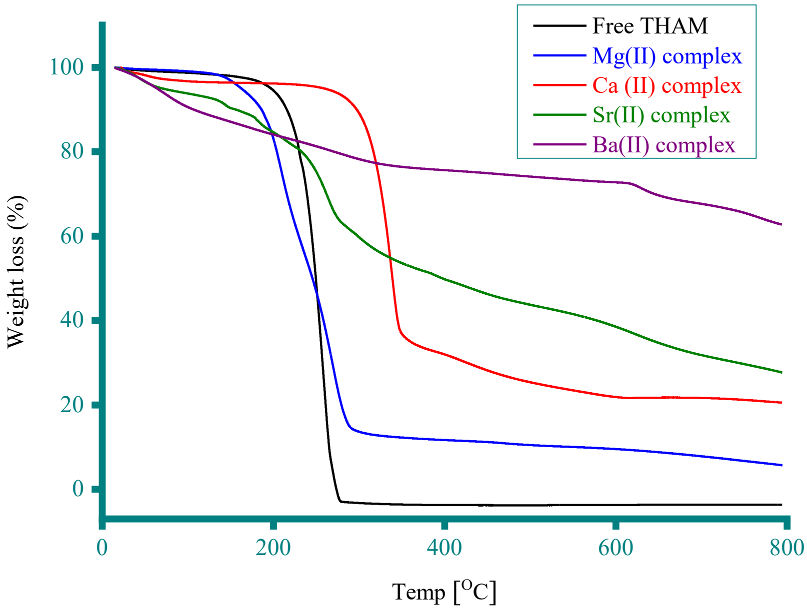

Fig. 5. Thermograms of free THAM, Ba(II), Ca(II), Sr(II),and Mg(II)complexes.

3.5 Structural morphologies

Scanning electron microscope (SEM) is the most frequently used technique for collecting specific outer surface-related information:

i- Surface topology.
ii- Microstructure and composition.
iii- Porous structure of the surface.

Surface morphologies of the synthesized complexes were pictured using a Quanta FEG 250 SEM instrument and are presented in Figure 6. These pictures were taken at different levels of magnification ranging from 2000 to x10,000. The SEM pictures of Ba(II), Ca(II), Sr(II), and Mg(II)complexes indicated that the particles of these complexes have a distinct size and morphology, and all have short rod-like morphology. This specific morphology was clearly observed for particles consisting Sr(II) and Mg(II) complexes. The rods of these two complexes were well-developed and had clear shapes, dimensions, and clear features. The short rod-like morphology was not obviously observed for particles of the Ca(II) and Ba(II) complexes. For a Ca(II) complex, several rods were broken into small pieces so that it appeared that these particles had no complete formation into rods. For Ba(II) complex, small granules were accumulated on the surface of a number of rods, indicating that a type of deformation had occurred to these rods. The particles of Mg(II) complex had a well-defined shape and a well-homogeneous and uniform matrix.

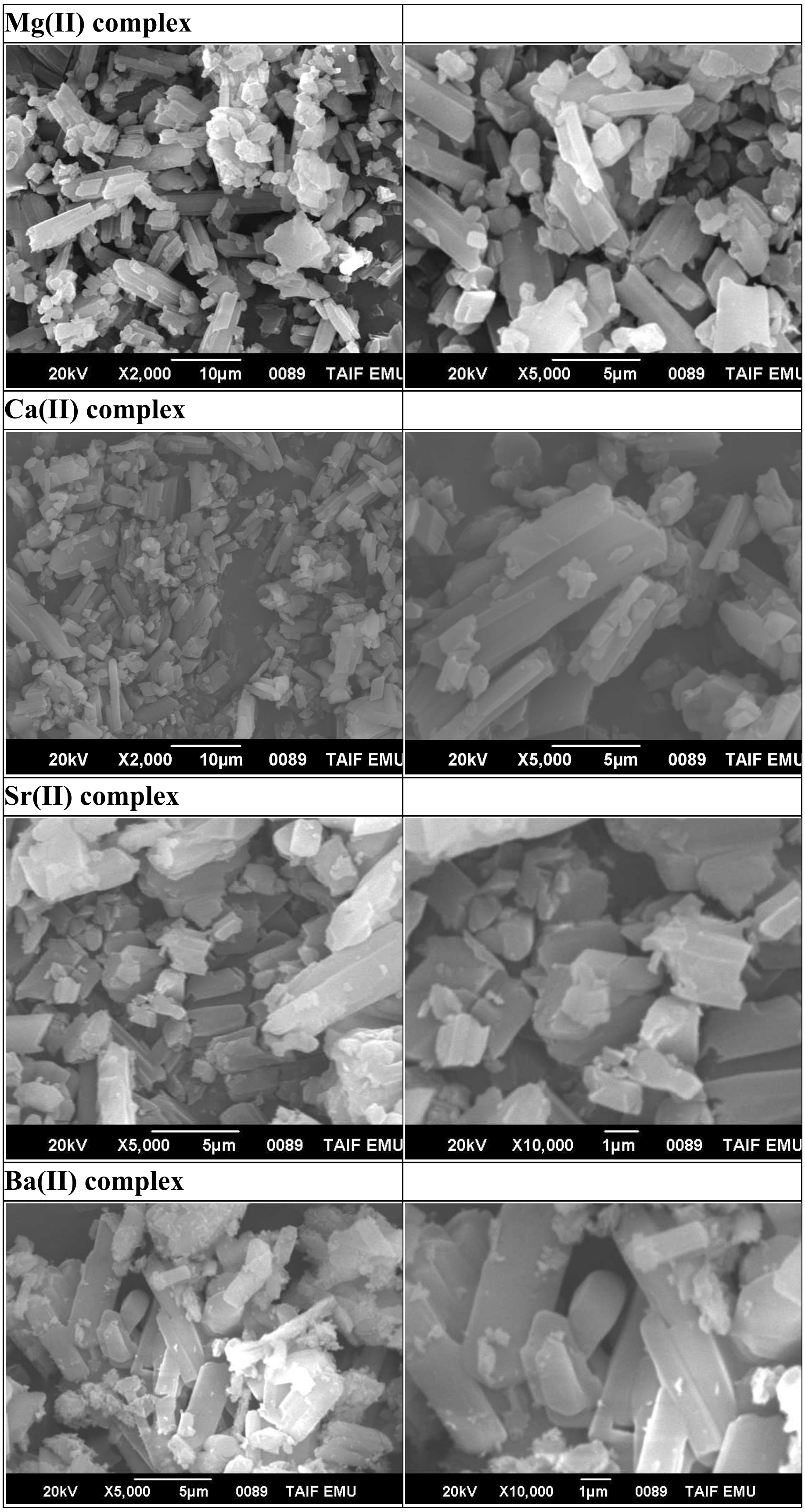

Fig. 6. SEM micrographs of Ba(II), Ca(II), Sr(II),and Mg(II) complexes.

4. Conclusion

Octahedral metal complexes of THAM with the ions Ba(II), Ca(II), Sr(II), and Mg(II) were prepared, and their structures were characterized using UV-visible, IR, Raman, and ^{1}H NMR spectroscopies and other physicochemical and analytical methods (elemental analysis, thermogravimetry, and SEM). Colorless products were obtained by the reaction of THAM with the metal ions with a stoichiometry of 2:1 (Ligand: Metal ion) at 65 °C and pH of ~8.5. Under these conditions, the THAM molecule ($C_4H_{11}NO_3$) losses a hydrogen atom and is transferred to the ($C_4H_{10}NO_3^-$; L^-) chelate with the metal ions forming colorless products. These products were formulated as $[BaL_2(H_2O)_2]$, $[CaL_2(H_2O)_2]\cdot2H_2O$, $[SrL_2(H_2O)_2]$, and $[MgL_2(H_2O)_2]\cdot4H_2O$, corresponding to the reaction of THAM with Ba(II), Ca(II), Sr(II), and Mg(II)ions, respectively. The morphology of the complexes was determined by SEM technique, and the obtained micrographs indicated that the complexes have short rod-like morphology.

ACKNOWLEDGEMENTS

This research was funded by the deanship of scientific research at Princess Nourah bint Abdulrahman University through the Fast–track Research Funding program.

References

Abdel Ghani, N.T. & Mansour, A.M. (2011) Novel Pd (II) and Pt (II) complexes of N, N-donor benzimidazole ligand: Synthesis, spectral, electrochemical, DFT studies and evaluation of biological activity. Inorganica Chimica Acta, 373, 249-258.

Abdel-Rahman, L.H., El-Khatib, R.M., Nassr, L.A.E., Abu-Dief, A.M., Mohamed, I. & Amin, A.S. (2014) Metal based pharmacologically active agents: Synthesis, structural characterization, molecular modeling, CT-DNA binding studies and *in vitro* antimicrobial screening of iron(II) bromosalicylidene amino acid chelates. Spectrochimica Acta A, 117, 366-378.

Albishri, H.M. & Marwani, H.M. (2016) Chemically modified activated carbon with tris (hydroxymethyl) aminomethane for selective adsorption and determination of gold in water samples. Arabian Journal of Chemistry, 9, S252-S258.

Alessio, E. (2011) Bioinorganic Medicinal Chemistry, Wiley-VCH Verlag GmbH and Co. KGaA.

Ali, F., Kamal, S., Shakeela, Q. and Ahmed, S. (2021) Extended-spectrumand Metallo-beta lactamase enzymesmediated resistance in Pseudomonas aeruginosa in clinically isolated specimens, Kuwait Journal of Science, 48(**2**), 1-10.

Asgedom, G., Sreedhara, A. & Rao, C.P. (1995) Oxovanadium(V) Schiff base complexes of tris(hydroxymethyl)aminomethane with salicylaldehyde and its derivatives: synthesis, characterization, and redox reactivity. Polyhedron, 14(**13-14**); 1995: 1873-1879.

Brignac, P.J. & Mo, C. (1975) Formation constants and metal-to-ligand ratios for tris(hydroxymethyl)aminomethane-metal complexes. Analytical Chemistry, 47(**8**), 1465-1466.

Bubb, W.A., Berthon, H.A. & Kuchel, P.W. (1995) Tris Buffer Reactivity with Low-Molecular-Weight Aldehydes: NMR Characterization of the Reactions of Glyceraldehyde-3-Phosphate. Bioorganic Chemistry, 23(**2**), 119-130.

Cao, Q., Li, Y., Freisinger, E., Qin, P.Z., Sigel, R.K.O. & Mao, Z-W. (2017) G-quadruplex DNA targeted metal complexes acting as potential anticancer drugs. Inorganic Chemistry Frontiers, 4, 10-32.

Chen, X., Wu, S., Yi, M., Ge, J., Yin, G. & Li, X. (2018) Preparation and physicochemical properties of blend films of feather keratin and poly (vinyl alcohol) compatibilized by tris (hydroxymethyl) aminomethane. Polymers, 10, 1054.

Crisóstomo-Lucas, C., García-Holley, P., Hernández-Ortega, S., Sánchez-Bartéz, F., Gracia-Mora, I. & Barba-Behrens, N. (2015) Structural characterization and cytotoxic activity of tioconazole coordination compounds with cobalt (II), copper (II), zinc (II) and cadmium (II). Inorganica Chimica Acta, 438, 245-254.

Dabrowiak, J.C. (2017) Metals in Medicine, 2nd ed., Wiley.

Dai, J., Dan, W., Ren, S., Shang, C. & Wang, J. (2018) Design, synthesis and biological evaluations of quaternization harman analogues as potential antibacterial agents. European Journal of Medicinal Chemistry, 160, 23-36.

Dasari, S. & Tchounwou, P.B. (2014) Cisplatin in cancer therapy: molecular mechanisms of action. European Journal of Pharmacology, 740, 364-378.

Deacon, G.B. & Phillips, R.J. (1980) Relationships between the carbon-oxygen stretching frequencies of carboxylato complexes and the type of carboxylate coordination. Coordination Chemistry Reviews, 33(3), 227-250.

Deng, Y., Wang, X-Z., Huang, S-H. & Li, C-H. (2019) Antibacterial activity evaluation of synthetic novel pleuromutilin derivatives in vitro and in experimental infection mice. European Journal of Medicinal Chemistry, 162, 194-202.

Dominelli, B., Correia, J.D.G. & Kühn, F.E. (2018) Medicinal applications of gold (I/III)-based complexes bearing N-heterocyclic carbene and phosphine ligands. Journal of Organometallic Chemistry, 866, 153-164.

El-Dissouky, A., Khalil, T.E., Elbadawy, H.A., El-Sayed, D.S., Attia, A.A. & Foro, S. (2020) X-ray crystal structure, spectroscopic and DFT computational studies of H-bonded charge transfer complexes of tris (hydroxymethyl)aminomethane (THAM) with chloranilic acid (CLA). Journal of Molecular Structure, 1200, 127066.

Galluzzi, L., Senovilla, L., Vitale, I., Michels, J., Martins, I., Kepp, O., Castedo, M. & Kroemer, G. (2012) Molecular mechanisms of cisplatin resistance. Oncogene, 31, 1869-1883.

Guidi, F., Modesti, A., Landini, I., Nobili, S., Mini, E., Bini, L., Puglia, M., Casini, A., Dyson, P.J., Gabbiani, C. & Messori, L. (2013) The molecular mechanisms of antimetastatic ruthenium compounds explored through DIGE proteomics. Journal of Inorganic Biochemistry, 118, 94-99.

Hambley, T.W. (2001) Platinum binding to DNA: structural controls and consequences. Journal of the Chemical Society, Dalton Transactions, 2711-2718.

Hayashi, N., Kinemuchi, H. & Kamijo, K. (1981) Effect of tris (hydroxymethyl) aminomethane on amine oxidase activity in dog brain, liver and serum and in human placenta. Japanese Journal of Pharmacology, 31(**5**), 737-746.

Howse, G.L., Bovill, R.A., Stephens, P.J. & Osborn, H.M.I. (2019) Synthesis and antibacterial profiles of targeted triclosan derivatives. European Journal of Medicinal Chemistry, 162, 51-58.

Hu, K., Zhou, G., Zhang, Z., Li, F., Li, J. & Liang, F. (2016) Two hydrazone copper (II) complexes: synthesis, crystal structure, cytotoxicity, and action mechanism. RSC Advances, 6, 36077-36084.

Kallet, R.H., Jasmer, R.M., Luce, J.M., Lin, L.H. & Marks, J.D. (2000) The treatment of acidosis in acute lung injury with tris-hydroxymethyl aminomethane (THAM). American Journal of Respiratory and Critical Care Medicine, 161(**4**), 1149-1153.

Khan, T-M., Gul, N.S., Lu, X., Wei, J-H., Liu, Y-C., Sun, H., Liang, H., Orvig, C. & Chen, Z-F. (2019) In vitro and in vivo anti-tumor activity of two gold (III) complexes with isoquinoline derivatives as ligands. European Journal of Medicinal Chemistry, 163, 333-343.

Köpf-Maier, P. (1994) Complexes of metals other than platinum as antitumour agents. European Journal of Clinical Pharmacology, 47, 1-16.

Lai, S., Jiang, G., Yao, J., Li, W., Han, B., Zhang, C., Zeng, C. & Liu, Y. (2015) Cytotoxic activity, DNA damage, cellular uptake, apoptosis and western blot analysis of ruthenium (II) polypyridyl complex against human lung decarcinoma A549 cell. Journal of Inorganic Biochemistry, 152, 1-9.

Lundblad, R.L. & Macdonald, F. (2010) Preparation of Buffers for Use in Enzyme Studies: G. Gomori, Handbook of Biochemistry and Molecular Biology, CRC Press, pp. 739-742.

Maheswari, P.U., Ster, M., Smulders, S., Barends, S., Wezel, G.P., Massera, C., Roy, S., Dulk, H., Gamez, P. & Reedijk, J. (2008) Structure, Cytotoxicity, and DNA-Cleavage Properties of the Complex [CuII(pbt)Br2]. Inorganic Chemistry, 47(**9**), 3719-3727.

Meng, T., Tang, S-F., Qin, Q-P., Liang, Y-L., Wu, C-X., Wang, C-Y., Yan, H-T., Dong, J-X. & Liu, Y-C. (2016) Evaluation of the effect of iodine substitution of 8-hydroxyquinoline on its platinum (II) complex: cytotoxicity, cell apoptosis and telomerase inhibition. MedChemComm, 7, 1802-1811.

Mjos, K.D. & Orvig, C. (2014) Metallodrugs in medicinal inorganic chemistry. Chemical Reviews, 114(**8**), 4540-4563.

Mohammed, Y.A., Baraki, T., Upadhyay, R.K. & Masood, A. (2014) Spectro-magnetic and antimicrobial studies on some 3d metal complexes with ethylenedianil of ortho-hydroxyphenylglyoxal. American Journal of Applied Chemistry, 2, 15-18.

Muhammad, N. & Guo, Z. (2014) Metal-based anticancer chemotherapeutic agents. Current Opinion in Chemical Biology, 19, 144-153.

Murakami, S., Sudo, Y., Miyano, K., Nishimura, H., Matoba, M., Shiraishi, S., Konno, H. & Uezono, Y. (2016) Tris-hydroxymethyl-aminomethane enhances capsaicin-induced intracellular Ca2+ influx through transient receptor potential V1 (TRPV1) channels. Journal of Pharmacological Sciences, 130(**2**), 72-77.

Nahas, G.G., Sutin, K.M., Fermon, C., Streat, S., Wiklund, L., Wahlander, S., Yellin, P., Brasch, H., Kanchuger, M., Capan, L., Manne, J., Helwig, H., Gaab, M., Pfenninger, E., Wetterberg, T., Holmdahl, M. & Turndorf, H. (1998) Guidelines for the treatment of acidaemia with THAM. Drugs, 55, 191-224.

Odabasoglu, M., Albayrak, Ç., Büyükgüngör, O. & Lönnecke, P. (2003) 2-{[Tris (hydroxymethyl) methyl] aminomethylene} cyclohexa-3, 5-dien-1 (2H)-one and its 6-hydroxy and 6-methoxy derivatives. Acta Crystallographica Section C, C59(**11**), o616-o619.

Pagoto, T.M.P., Sobrinho, L.L.G., Graminha, A.E., Guedes, A.P.M., Carroccia, M.C., de Oliveira, P.F., Silveira-Lacerda, E.P., Deflon, V.M., Tavares, D.C., Pivatto, M., Batista, A.A. & Poelhsitz, G.V. (2015) A ruthenium (II) complex with the propionate ion: Synthesis, characterization and cytotoxic activity. Comptes Rendus Chimie, 18(**12**), 1313-1319.

Qin, Q-P., Wang, S-L., Tan, M-X., Liu, Y-C., Meng, T., Zou, B-Q. & Liang, H. (2019) Synthesis of two platinum (II) complexes with 2-methyl-8-quinolinol derivatives as ligands and study of their antitumor activities. European Journal of Medicinal Chemistry, 161, 334-342.

Saleem, K., Wani, W.A., Haque, A., Lone, M.N., Ali, I., Ming-Fa, H. & Jairajpuri, M.A. (2013) Synthesis, DNA binding, hemolysis assays and anticancer studies of copper (II), nickel (II) and iron(III) complexes of a pyrazoline-based ligand, Future Medicinal Chemistry, 5, 135-146.

Sayadi, M., Sabounchei, S.J., Sedghi, A., Bayat, M., Hosseinzadeh, L. & Gable, R.W. (2019) Synthesis, characterization, theoretical and cytotoxicity studies of Pd (II) and Pt (II) complexes with new bidentate carbon donor ligand. Polyhedron, 161, 179-188.

Singh, U., Malla, A.M., Bhat, I.A., Ahmad, A., Bukhari, M.N., Bhat, S., Anayutullah, S. & Hashmi, A.A. (2016) Synthesis, molecular docking and evaluation of antifungal activity of Ni(II), Co(II) and Cu(II) complexes of porphyrin core macromolecular ligand. Microbial Pathogenesis, 93, 172-179.

Tarafder, M.H.T., Saravanan, N., Crouse, K.A. & Ali, A.M. (2001) Coordination chemistry and biological activity of nickel(II) and copper(II) ion complexes with nitrogen–sulphur donor ligands derived from S-benzyldithiocarbazate (SBDTC). Transition Metal Chemistry, 26, 613-618.

Tatar, L., Nazır, H., Gümüşer, M., Kale, C. & Atakol, O. (2005) Synthesis, crystal structure and electrochemical behaviour of water soluble Schiff bases. Zeitschrift für Kristallographie – Crystalline Materials, 220(**7**), 639-642.

Tavares, T.T., Azevedo, G.C., Garcia, A., Carpanez, A.G., Lewer, P.M., Paschoal, D., Müller, B.L., Dos Santos, H.F., Matos, R.C., Silva, H., Grazul, R.M. & Fontes, A.P.S. (2017) Gold(I) complexes with aryl-thiosemicarbazones: Molecular modeling, synthesis, cytotoxicity and TrxR inhibition. Polyhedron, 132, 95-104.

Tella, A.C., Obaleye, J.A., Olawale, M.D., Ngororabanga, J.M.V., Ogunlaja, A.S. & Bourned, S.A. (2019) Synthesis, crystal structure, and density functional theory study of a zinc(II) complex containing terpyridine and pyridine-2,6-dicarboxylic acid ligands: Analysis of the interactions with amoxicillin. Comptes Rendus Chimie, 22(**1**), 3-12.

Trudu, F., Amato, F., Vaňhara, P., Pivetta, T., Peña-Méndez, E.M. & Havel, J. (2015) Coordination compounds in cancer: Past, present and perspectives. Journal of Applied Biomedicine, 13(**2**), 79-103.

Vakili, S., Asadikaram, G., Torkzadeh-Mahani, M., Behroozikhah, A., Nematollahi, M.H. & Savardashtaki, A. (2021) Design and construction of a localized surface plasmon resonance-based goldnanobiosensor for rapid detection of brucellosis, Kuwait Journal of Science, 48(**3**), 1-9.

Walsh, T.R., Efthimiou, J. & Dréno, B. (2016) Systematic review of antibiotic resistance in acne: an increasing topical and oral threat. Lancet Infectious Diseases, 16, e23-e33.

Weber, T., Tschernich, H., Sitzwohl, C., Ullrich, R., Germann, P., Zimpfer, M., Sladen, R.N. & Huemer, G. (2000) Tromethamine buffer modifies the depressant effect of permissive hypercapnia on myocardial contractility in patients with acute respiratory distress syndrome. American Journal of Respiratory and Critical Care Medicine, 162(**4**), 1361-1365.

WHO, (2016) Tacking drug-resistant infections globally: final report and recommendations.

Submitted: 16/11/2020
Revised: 28/11/2020
Accepted: 10/08/2021
DOI: 10.48129/kjs.11047